Distal Val346Ile Mutation in Inducible NO Synthase Promotes Substrate-Dependent NO Confinement†

Edward Beaumont,‡ Jean-Christophe Lambry,‡ Zhi-Qiang Wang,§ Dennis J. Stuehr,|| Jean-Louis Martin,‡ and Anny Slama-Schwok*,‡

INSERM U696, Laboratory of Optics and Biosciences, CNRS UMR 7645, Ecole Polytechnique, 91128 Palaiseau, France, Department of Chemistry, Kent State University Tuscarawas, New Philadelphia, Ohio 44663, and Department of Pathobiology, Lerner Research Institute, Cleveland Clinic Foundation, Cleveland, Ohio 44195

Received August 6, 2007; Revised Manuscript Received September 21, 2007

ABSTRACT: The function of inducible NO synthase (WT iNOS) depends on the release of NO from the ferric heme before the enzyme is reduced. Key parameters controlling ligand dynamics include the distal and proximal heme pocket amino acids, as well as the inner solvent molecules. In this work, we tested how a point mutation in the distal heme side of WT iNOS affected the geminate rebinding of NO by ultrafast kinetics and molecular dynamics simulations. The mutation sequestered much of the photodissociated NO close to the heme compared to WT iNOS, with a main picosecond phase accounting for 78% of the rebinding to the arginine-bound Val346Ile protein. Consequently, the probability of NO release from Val346Ile decreased as compared to that from WT iNOS, provided the substrate binding site is filled. These data are rationalized by a steric effect of the Ile methyl group inducing events mediated by the substrate, transmitted via the propionates to the NO and the protein. This model is consistent with the role of the H-bonding network involving the heme, the substrate, and the BH_4 cofactor in controlling NO release, with a key role of the heme propionates [Gautier et al. (2006) *Nitric Oxide 15*, 312]. These data support the effect of Val346Ile mutation in decreasing NO release and slowing down NO synthesis compared to WT iNOS determined by single turnover catalysis [Wang et al. (2004) *J. Biol. Chem. 279*, 19018].

The dissociation of the NO ligand from the NO-synthase (NOS) enzymes is a critical step in regulating their activity, since the newly formed NO must be released from the ferric heme before onset of the next catalytic cycle (*1*, *2*). Factors influencing the release of NO from the heme before the enzyme gets reduced are thus of particular relevance for function. The iron−NO bond is generally photolabile in hemoproteins and can be dissociated with a laser pulse, and the subsequent dynamics of NO rebinding to the heme along with the associated protein changes can be monitored within picoseconds to nanoseconds (*3*, *4*). Key parameters controlling ligand dynamics include the distal and proximal heme pocket amino acids, as well as inner solvent molecules (*3*−*8*). Rebinding of diatomic heme ligands to the heme have been extensively studied with myoglogin (Mb[1]) as a "prototype protein" (*3*, *4*, *6*−*8*). The rates of ligand rebinding following photolysis were sensitive to mutation of distal residues. These effects were attributed to changes in free volume and steric hindrance in the heme pocket (*9*). For example, bulky mutations at Val68 regulated access to the heme iron and to a nearby xenon cavity (*10*). Indeed, ligand dynamics in myoglobin is associated with pre-existing internal protein cavities, shown to bind xenon (*4*). Recently, the role of heme propionates in the dissipation of the excess energy of the heme and information transmission to the myoglobin protein following photodissciation of the ligand has been emphasized by molecular dynamics and Raman spectroscopy (*11*−*13*). Thus, geminate recombination allows probing the heme environment and testing the effect of point mutations in its vicinity.

In this work, we study the effect of the mutation Val346 to Ile on the NO rebinding to the oxygenase domain of WT iNOS. This mutation is located at the distal heme side and may restrict NO diffusion to the heme by steric hindrance of the additional methyl group of Ile with respect to Val. Replacement of Val346 by Ile was found to slow down the k_{on} rates of NO by comparison with the rates determined for wild-type WT iNOS (*14*). Moreover, this mutation also decreased Fe(III)−NO dissociation rate in the single turnover catalytical reaction by 3 times (*14*). In all bacterial NOS-like proteins, the distal valine residue of the mammalian NOS enzymes is always replaced by isoleucine (*14*−*19*). In our previous work (*20*), we measured a faster rate of NO geminate recombination in the bacterial NOS-like proteins

† This work was supported by an MRT fellowship to E.B. from the French Ministry for Research and Education and by NIH Grant CA53914 to D.J.S.

* Corresponding author. Tel: 33-1-69335061. Fax: 33-1-69335084. E-mail: Anny.Schwok@gmail.com.

‡ Ecole Polytechnique.

§ Kent State University Tuscarawas.

|| Cleveland Clinic Foundation.

[1] Abbreviations: WT iNOS, inducible NO-synthase; V346I, mutation of the Val346 residue of iNOS into Ile346; Mb, myoglogin; SA-HNS, bacterial NOS-like proteins of *Staphylococcus aureus*; BA-HNS, NOS-like protein from *Bacillus anthracis*; NOHA, *N*-hydroxyarginine; BH_4, (6*R*)-5,6,7,8-tetrahydrobiopterin; SVD, singular matrix decomposition of the time-wavelength matrix.

10.1021/bi701567h CCC: $37.00
Published on Web 10/31/2007

of *Staphylococcus aureus* (SA-HNS) compared to the NO rebinding rate in eNOS and in the NOS-like protein from *Bacillus anthracis* (BA-HNS) with the presence of substrate. These differences were attributed to higher energy barriers between the heme and a second NO binding site in SA-HNS compared to BA-HNS. Interestingly, these differences between the bacterial proteins were diminished in the absence of arginine, suggesting a dynamic role of the substrate binding. Since both proteins carry the Ile residue and yet the NO dynamic differed, the steric effect of the Ile compared to a Val could not be rigorously evaluated. In the present work, we tested the effect of the V346I mutation on NO geminate recombination to the ferric proteins by combining ultrafast kinetics monitoring and molecular dynamic simulations. The NO geminate rebinding rates in V346I were enhanced in the presence of arginine or *N*-hydroxyarginine (NOHA) as compared to that in WT iNOS. However, the effect of the mutation was abolished in the absence of the substrate, suggesting that substrate-mediated steric changes are critical for the geminate recombination of NO to the heme. The absence of substrate modified the interactions of NO with the heme by changing the Fe−NO bond, altering the H-bonding network linking the heme, BH_4 cofactor, and many conserved residues in the near vicinity (*20*−*22*). Molecular modeling identified that the steric effect of the Ile substitution could be mediated by coupled fluctuations of the substrate, the heme propionates, and NO, altering the H-bonding interactions in the mutated protein. Such a network seemed critical for intramolecular signal transduction in WT iNOS, as recently reported in myoglobin (*12*).

EXPERIMENTAL PROCEDURES

Materials. L-Arginine, (6*R*)-5,6,7,8-tetrahydrobiopterin (BH_4), chemicals used for the Tris buffer, hydroxyarginine (NOHA), potassium ferricyanide, and glycerol were purchased from Sigma. NO gas and high-purity argon (99.9995%) were obtained from Air Product.

Expression of the Enzymes. Wild-type and mutant V346I oxygenase domain of Δ 65 iNOS proteins (amino acids 66−498 plus a six His-tag extension at the C-terminus) were overexpressed in BL21 cells using the pCWori vector and purified as reported previously (*14*).

Sample Preparations for Spectroscopy. A concentrated solution of wild-type iNOSoxy or its V346I mutant in 50 mM HEPES buffer (pH = 7.5) and 5% glycerol was mixed with 1 mM arginine, or NOHA, or in the absence of substrate (as indicated) in a optical cuvette with an 1 mm path length. It was sealed with a rubber stopper and degassed by repetitive cycles of vacuum and argon. Anaerobic solutions of 1 mM BH_4 were then added to the protein. The concentration of BH_4 was determined by its absorbance at 298 nm ($\epsilon_{298} = 9.4 \times 10^3\ M^{-1}\ cm^{-1}$). The solution was then incubated overnight on ice to allow completeness of the equilibration. 10% NO gas (100% NO diluted in argon supplied by Air Product) was then introduced in the cell at a pressure of 1.3 bar using a gas train.

Time-Resolved Spectroscopy. Time-resolved spectroscopy was performed with a 30 Hz pump−probe laser setup described previously (*23*). Photodissociation of NO-bound WT iNOS was achieved by an excitation pulse at 565 nm with a pulse width of 40 fs. The transient spectrum detected after a variable delay was probed with a white light continuum pulse, whose group velocity dispersion was minimized at 400 nm by a set of prisms. The wavelength calibration of the CCD camera was checked every day by using a thin-bands filter. Twenty-five scans were simultaneously recorded in two time windows: 10 and 500 ps, or 50 ps and 3 ns. Carbon monoxide bound to reduced myoglobin was monitored under the same conditions and used as reference of flat kinetics in the time scales of 500 ps to 4 ns (*23*). Analysis of the data was performed by singular matrix decomposition (SVD) of the time−wavelength matrix (*24*).

Molecular Dynamics Simulations. The modeling was performed using the CHARMM32 software on a HPJ5600 computer. The calculations used the PDB file 1NSI (*25*). The dimer is composed of two identical chains of 431 residues each, two iron protoporphyrins, one Zn atom at the dimer interface, two NO ligands, two BH_4 and arginine molecules, and 279 water molecules from the X-ray data to which a "bath" of 4035 water molecules was added (*26*). Hydrogen atoms were generated using the CHARMM HBUILD command. The energy of the structure was minimized. A relative dielectric constant equal to unity was applied to the entire structure. The equations of motion were numerically integrated using the Verlet algorithm with 1 fs time steps. To prepare simulations, an initial heating from 0 to 300 K and equilibration at 300 K were performed with atoms velocities calculated according to a Maxwell distribution. Several free dynamic 50 ps runs were performed to obtain stable starting structure(s) before the NO dissociation. To simulate NO dissociation, the sudden approximation was used, by deleting the Fe−NO bond and switching to deoxyheme parameters. A three-point charge model was used for dissociated NO (*27*). Four trajectories of 50 or 100 ps, representing eight dissociation events, were performed for WT iNOS and V346I mutant.

RESULTS

(I) Effect of the Mutation on the NO Rebinding to the Heme: Steady-State Absorption. Both oxygenase domains of WT iNOS and its V346I mutant (V346I) are predominantly in a low-spin state with their Soret band peak around 420 nm in the absence of substrate and the cofactor BH_4. Interestingly, arginine was slightly more efficient than *N*-hydroxyarginine (NOHA) in promoting the low-spin to high-spin conversion of V346I (left panel of Figure 1 and ref *28*). In contrast, binding of both substrate and NOHA affected similarly WT iNOS spin status. Binding of both substrate and cofactor to WT iNOS or its mutant induced a blue-shift of the Soret band to 396 nm, indicating the high spin of the heme. The ferric nitrosyl complexes of both proteins peaked at 440 ± 1 nm. Evidence for the formation of the nitrosyl complex is given by the difference spectra (ferric − ferric-NO) presented in the right panel of Figure 1. Extrema were observed at 396 nm and 442 ± 1 nm for both proteins.

Transient Absorption. The kinetics of photoinduced release and rebinding of NO from the ferric nitrosylated WT iNOS and its mutant was measured by ultrafast absorption spectroscopy. We used a short pump pulse at wavelength 565 nm to selectively cleave the Fe−NO bond of the ferric nitrosyl complex within 40 fs. Then a probe beam monitored

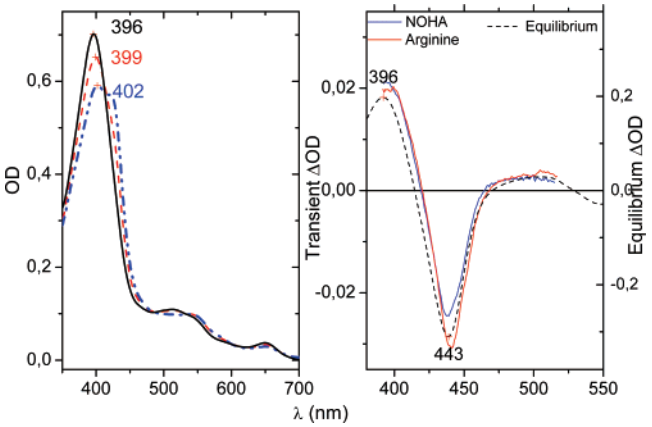

FIGURE 1: (Left panel) Effect of the substrate on the equilibrium absorption spectrum of V346I: solid, 1 mM arginine + 1 mM BH_4; dashed red, 1 mM arginine; dashed and dotted blue, 1 mM NOHA, both in the absence of BH_4. (Right panel) Comparison of the absorption difference spectra at equilibrium of Fe(III) minus the Fe(III)NO complex of V346I (right scale, dashed) and the transient one recorded 50 ps after the pump (left scale, solid lines) [V346I] = 65μM, 1 mM arginine + 1 mM BH_4, 50 mM Tris (pH = 7.5), 150 mM NaCl in a 1 mm path optical cell. The slight shifts of the extrema between equilibrium and transient difference spectra are within experimental error.

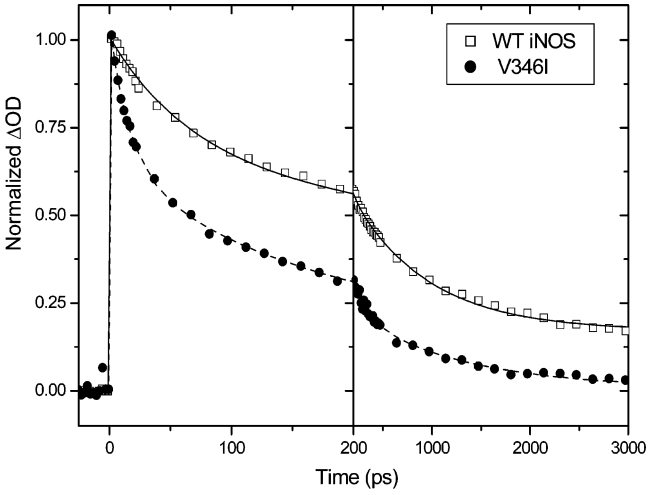

FIGURE 2: Effect of the Val346Ile mutation on NO rebinding to the heme with NOHA bound. The main SVD components are normalized and presented on 200 ps and 3 ns time scales for WT iNOS (open squares) or V346I mutant (full circles) in the presence of 1 mM NOHA and 1 mM BH_4. Other conditions are the same as in Figure 1B. The ferric nitrosyl complexes were equilibrated with 10% NO in the gas phase (200 μM). The fitting curves are shown as solid or dashed lines, and fitting data are given in Table 1.

the evolution of the absorption spectrum after cleavage of the bond with high time resolution. A typical NO rebinding kinetics to the heme following its photodissociation is shown in Figure 2. The amplitude ΔOD was proportional to the difference ΔOD(t=0) = [Fe(III)] − [Fe(III)−NO]; when the signal reached 0, all NO were rebound to the heme. The right panel of Figure 1 shows that the transient spectrum monitored 50 ps after the pump beam was very similar to the difference spectrum obtained at equilibrium. This indicated geminate rebinding. This process involved the same laser-dissociated NO ligand remaining in the protein and rebinding to the heme within picoseconds to nanoseconds. The geminate recombination is often a multiphasic process (*3*, *6*, *9*−*11*, *20*, *22*−*23*). This process involved a picosecond step due to the rebinding of NO that did not escape the heme vicinity after photodissociation and is often activationless (*20*). The nanosecond step phase reflected the rebinding of NO molecules dissociated with excess energy from the protein to the heme pocket but still remaining in the protein, corresponding to ground-state processes. The latter step was generally associated with overcoming of internal energy barrier(s), alternatively assigned to ligand migration (*3*−*10*, *20*). The upper limit of the probability of NO escape from the protein was given by the asymptotic value, corresponding to NO ligands remaining unbound in 3−5 ns.

NO rebinding to WT iNOS was measured in the presence of the cofactor BH_4 and *N*-hydroxyarginine (NOHA). The decay was best fitted by three exponentials, τ_1= 34 ± 4 ps (20%), τ_2= 186 ± 25 ps (28%), and τ_3= 1200 ± 200 ps (39%), and a constant (Figure 2 and Table 1). The kinetics of NO recombination to the mutated enzyme was faster, with a main picosecond phase accounting for 78% of the signal and characterized by τ_1= 16 ± 2 ps (37%), τ_2= 150 ± 20 ps (41%). It was followed by a small nanosecond phase τ_3= 1130 ± 180 ps (23%) and a negligible constant term. The main effect of the Val−Ile mutation was therefore mainly noticeable in the fast picosecond component. During this short picosecond time frame, NO rebinding occurred in close vicinity to the heme. The mutation also decreased the probability of NO release from V346I as compared to that from WT iNOS, as judged by the constant values (Table 1), suggesting induced changes in ligand migration (within the protein).

(II) Effect of the Substrate on Ultrafast NO Rebinding in WT iNOS and V346I. NO rebinding in WT iNOS and V346I were measured in the presence NOHA or arginine (Figure 3 and Table 1). In WT iNOS, only modest changes in the geminate rebinding rate were observed by switching from NOHA to arginine: it mainly decreased the amplitude of the first picosecond component from A_1= 0.20 to 0.12, respectively. The nanosecond lifetime increased from τ_3= 1200 ± 100 ps (NOHA) to τ_3= 1850 ± 200 ps (arginine), and the constant value decreased accordingly (Table 1). Figure 3 shows that NO rebinding to V346I was affected by substituting NOHA with arginine. The first lifetime increased from τ_1= 16 ± 2 ps to τ_1= 25 ± 3 ps. A significant rise of the constant value from 0.01 to 0.09, respectively, was also observed (Table 1); thus, opposite effects of replacing NOHA by arginine were obtained on WT iNOS and V346I.

To test these effects further, the geminate rebinding of NO in V346I and WT iNOS was measured in the absence of substrate. In these conditions, removal of the guanidinium group of the arginine substrate may minimize any steric hindrance. Indeed, Figure 4 showed that NO rebinding to the heme became very similar in both WT and mutated protein in the absence of substrate. The kinetics in the absence of substrate presented a similar nanosecond component, τ_3 = 738 ± 90 ps (V346I) and τ_3= 848 ± 95 ps (WT iNOS), accounting for ca. 55% decay. The amplitudes of picosecond components significantly decreased in V346I in the absence of arginine (Figures 3 and 4). The probability of NO release from the mutated protein remained unchanged on the nanosecond time scale, as judged by the similar A_4 values with or without arginine. In contrast, the absence of substrate bound to WT iNOS mainly shortened the nanosecond lifetime from τ_3 =1850 ± 180 ps (with arginine) to

Table 1: Effect of the Substrate on NO Rebinding to the Heme in the Presence of BH_4 at 20 °C[a]

sample	arginine	NOHA	$\tau_1 \pm 10\%$ (ps)	A_1[b]	$\tau_2 \pm 10\%$ (ps)	A_2[b]	$\tau_3 \pm 10\%$ (ps)	A_3[b]	A_4[b]
WT iNOS	−	−	33	0.10	145	0.31	848	0.54	0.05
	+	−	37	0.12	314	0.51	1850	0.31	0.06
	−	+	34	0.20	186	0.28	1200	0.39	0.14
V346I	−	−	28	0.14	121	0.25	738	0.55	0.08
	+	−	25	0.43	87	0.34	1016	0.14	0.09
	−	+	16	0.37	150	0.41	1130	0.23	0.01

[a] The experiments were performed (in duplicate or triplicate) with 60−70 μM of the oxygenase domain of the proteins in the presence of 10% NO in the gas phase. [b] Relative amplitude ($A_1 + A_2 + A_3 + A_4 = 1$); the error on the amplitudes is ±13%.

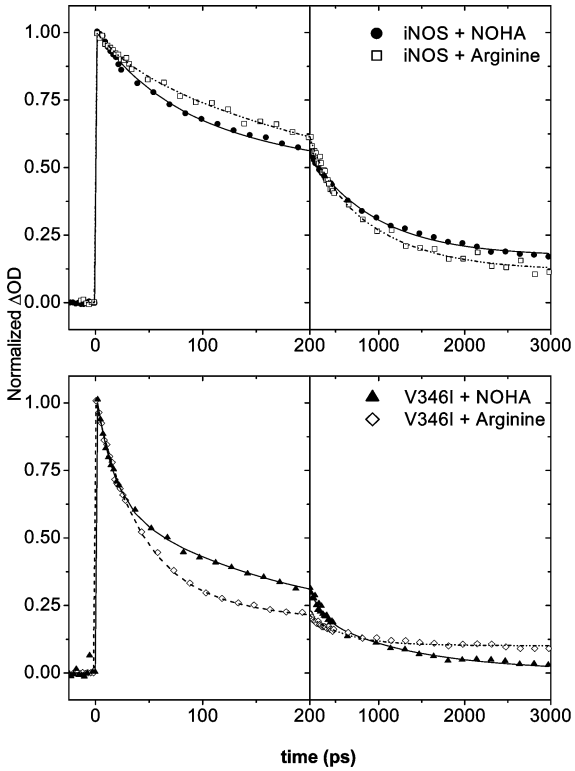

FIGURE 3: Different effects of the arginine or NOHA bound to the substrate site on NO rebinding to the ferric heme of WT iNOS (upper panel) and V346I (lower panel), 1 mM substrate, and BH_4, under the same conditions as in Figure 1B: ● and full line, WT iNOS + NOHA; □ and dashed line, WT iNOS + arginine; ▲ and solid line, V346I + NOHA; ◇ and dashed line: V346I + arginine.

850 ± 90 ps (without arginine); it also shortened the decay on the picosecond time scale from $\tau_2 = 314 \pm 35$ ps (with arginine) to 145 ± 20 ps in the absence of arginine. Thus, NO rebinding to V346I heme was much slower in the absence than in the presence of arginine, while the overall NO released from the protein (proportional to the constant value) remained unchanged. This suggested additional effects besides steric hindrance.

Figure 5 and Table 2 show the temperature dependence of NO rebinding to the heme, which was quite weak for WT iNOS in the presence of arginine (Table 2). In contrast, the NO rebinding in the mutated protein presented a larger effect of the temperature. A large decrease of the amplitude A_2 in the second recombination step was compensated by an increase of the amplitude A_3 of the nanosecond component, leading to a similar overall escape probability of NO from the mutated V346I. This suggested that thermal fluctuations in the heme pocket conformation were more important in V346I as compared to WT iNOS. To get a better understanding of these effects, molecular dynamic simulations were performed in both WT iNOS and V346I in the presence of arginine.

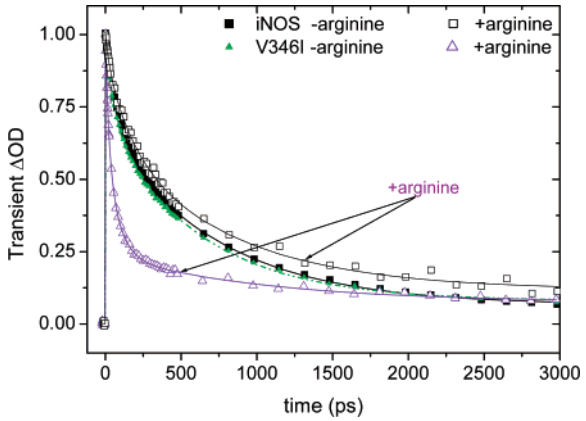

FIGURE 4: Effect of the Val346Ile mutation on the NO rebinding in the absence of substrate. Comparison of the main SVD component in WT iNOS + arginine (□), WT iNOS − arginine (■), V346I + arginine (△), V346I − arginine (▲). Other conditions are same as in Figure 1B.

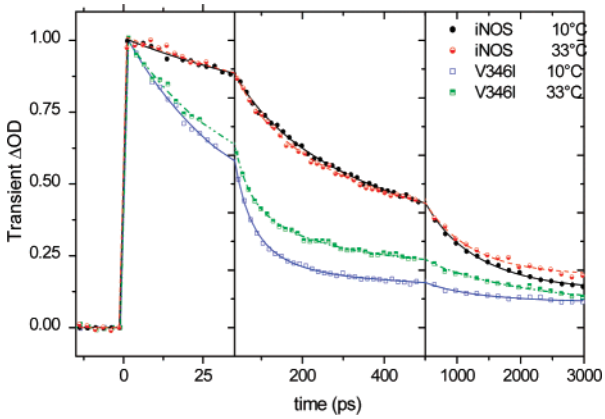

FIGURE 5: Effect of the temperature on NO geminate rebinding in WT iNOS or V346I. Note the small effect of increasing the temperature from 10 to 33 °C on NO rebinding in WT iNOS (arginine-bound) (black and red circles, respectively). In contrast, the same temperature increase induced more noticeable effects on NO rebinding to V346I (open and full squares, respectively). Both proteins are repleted with BH_4. The fit of the data are listed in Table 2.

(III) Molecular Modeling in Both WT iNOS and V346I Mutant. Simulations of the dynamics of NO rebinding were performed using the structure of BH_4-bound WT iNOS referred to as 1NSI in the PDB as a starting point (*25*−*27*). The Ile mutant was generated by adding a methyl group to the Val346 residue. Ile346 adopted a similar conformation as that found in bsNOS, with the methyl group pointing down

Table 2: Effect of Temperature on NO Rebinding to the Ferric Heme in the Presence of Arginine and BH_4[a]

sample	T (°C)	$\tau_1 \pm 16\%$ (ps)	A_1[b]	$\tau_2 \pm 10\%$ (ps)	A_2[b]	$\tau_3 \pm 10\%$ (ps)	A_3[b]	A_4[b]
WT iNOS	10	54	0.15	345	0.45	1704	0.31	0.09
	20	37	0.12	314	0.51	1850	0.31	0.06
	33	65	0.19	280	0.44	1990	0.27	0.11
V346I	10	30	0.45	79	0.35	883	0.11	0.09
	20	24	0.43	87	0.34	1016	0.14	0.09
	33	32	0.49	128	0.23	1300	0.20	0.08

[a] The experiments were performed (in duplicate or triplicate) with 60−70 μM of the oxygenase domain of the proteins in the presence of 10% NO in the gas phase. [b] Relative amplitude ($A_1 + A_2 + A_3 + A_4 = 1$); the error on the amplitudes is ±13%.

the heme (*17*). Figure 6 shows the structure of WT iNOS heme in the presence of arginine represented in green. The structures included the bound pterin (not shown in the figure). Superimposed is the structure simulated in the mutated protein depicted in orange (Figure 6A). The two structures differed by a number of related parameters. First, the position of the substrate was found in an H-bonding distance from the heme propionate in WT iNOS. This distance was very stable in many trajectories at $d = 2.8$ Å. In contrast, the same distance was fluctuating in the mutated protein between two conformations (Figure 6B) [Extending the first 250 ps of free dynamics (before NO dissociation) by an additional 100 ps did not change the results.] The distribution of the propionate A torsion angle was broad, varying between 120° and 180° as compared to a representative value of 150° in WT iNOS. Additionally, the distance between the arginine substrate and the heme propionate A in the mutated protein changed from 2.7 Å to ≈5.0 Å (Figure 6B). From these calculations, both the H-bonded and nonbonded conformations seem likely; sharp transitions between these two states were observed in the dynamics (following dissociation, data not shown). The simulations also suggest that one water molecule located just in between the propionates may participate in this interaction (Figure 6A). Thus, the methyl group of Ile346 seemed to induce events, mediated by the substrate binding, transmitted via the propionates to the NO and the protein.

DISCUSSION

(a) Effect of the Val/Ile Mutation in the Presence/Absence of Substrate. Geminate rebinding of NO in V346I was much faster than in WT iNOS in the presence of substrate and BH_4 (Figure 4). The extensive NO rebinding observed already on the picosecond time scale indicated structural and/or dynamic changes induced by the mutation in the immediate vicinity of the heme iron. The methyl group only accounts for 10 Å^3, which afforded a modest reduction of the free volume of the distal heme pocket (*14*). However, the added methyl group was located close to the heme and to bulky aromatic residues and may sequester NO close to the heme (*16*, *17*). This confinement of NO in the protein was proposed to account for the decrease of the rate of Fe(III)−NO dissociation from $k_{off} = 20.7$ s^{-1} (WT iNOS) to 1.9 s^{-1} (V346I), as well as the bimolecular rate of ferric nitrosyl formation, from $k_{on} = 0.27$ to 0.033 μM^{-1} s^{-1}, respectively (*14*). All these rates were obtained in the presence of NOHA. They agree well with the calculated rate of NO release from Fe(III)−NO deduced from single-turnover reactions: 2.3 ± 0.1 and 0.77 ± 0.03 s^{-1} for WT iNOS and V346I, respectively. These differences are consistent with the data reported in this work, provided the substrate site is filled with NOHA (Figures 2 and 4). The effect of the mutation extended to the nanosecond phase, and a decreased NO escape from the protein was observed in the mutated enzyme compared to the wild-type. Thus, NO diffusion in the protein to potential "docking sites" was largely eliminated and the probability of NO release from the mutated protein was close to 0 as compared to 0.14 in WT iNOS in the presence of NOHA. Mutations in the distal heme residues of myoglobin were previously reported to modify the nanosecond component of the geminate recombination (*6*−*11*, *23*).

Switching from NOHA to arginine resulted in opposite variation of A_4 values in WT iNOS and V346I. In WT iNOS, the small decrease in A_4 dropping from 0.14 to 0.06, respectively, by switching from NOHA to arginine was consistent with a 2-fold decrease in k_{off} (*14*, *29*). This could reflect the different steric hindrance of arginine as compared to the tightly constrained NOHA and showed that the catalytic heme site is nicely fitted for an optimal recognition of the substrate in WT iNOS (*30*). In the mutated protein, the potential "docking sites" were slightly more accessible for NO diffusion when arginine was bound compared to that observed with NOHA: the decrease of A_3 and concomitant increase in A_4 values suggested that the effect of the mutation propagates to larger distances in arginine-repleted V346I.

To test whether removal of the substrate would reduce the steric hindrance to NO rebinding induced by the Ile extra methyl group, we performed two sets of experiments. First, we used molecular dynamics simulations to get a closer insight on the structural dynamics in both WT and mutated proteins; second, we tested the effect of temperature on NO rebinding to WT iNOS and V346I, with the hypothesis that steric effects may be reduced or abrogated at higher temperatures. The simulations shown in Figure 6 supported the steric effects of the mutation resulting from indirect interactions in the distal heme side. The substrate position was largely fluctuating in V346I as compared to the tight arginine binding in WT iNOS, even at 20 °C. Indeed, the H-bonding network involving the substrate, NO, and the propionates are known in NOS in general and in WT iNOS in particular (*2*, *21*, *25*, *31*). This network kept the arginine in a well-defined and rather fixed conformation in WT iNOS. In the mutated protein, the higher mobility of the substrate was linked to the presence of the Ile methyl group (Figure 6A). The simulations also showed that the fluctuations in the substrate binding mode were coupled with the rotation of the propionate groups, reaching two distinct conformations (Figure 6A,B). The fluctuations between them were observed on the 50−100 ps time scale of the simulations and alternatively abolished the H-bond found between arginine and the propionate in V346I (data not shown (*21*)). Experimentally, they likely contributed to NO rebinding in the first ca. 200 ps (Figures 2−4).

H-bonding interactions involving the propionate groups were known to affect the geminate recombination (*32*). Propionates helped dissipating heme excess energy within ca. 7 ps after ligand photodissociation by coupling with solvent molecules (*11*, *13*); this is likely not to be the major effect of the mutation observed at longer time scales. The dynamics of the coupled fluctuations of the substrate,

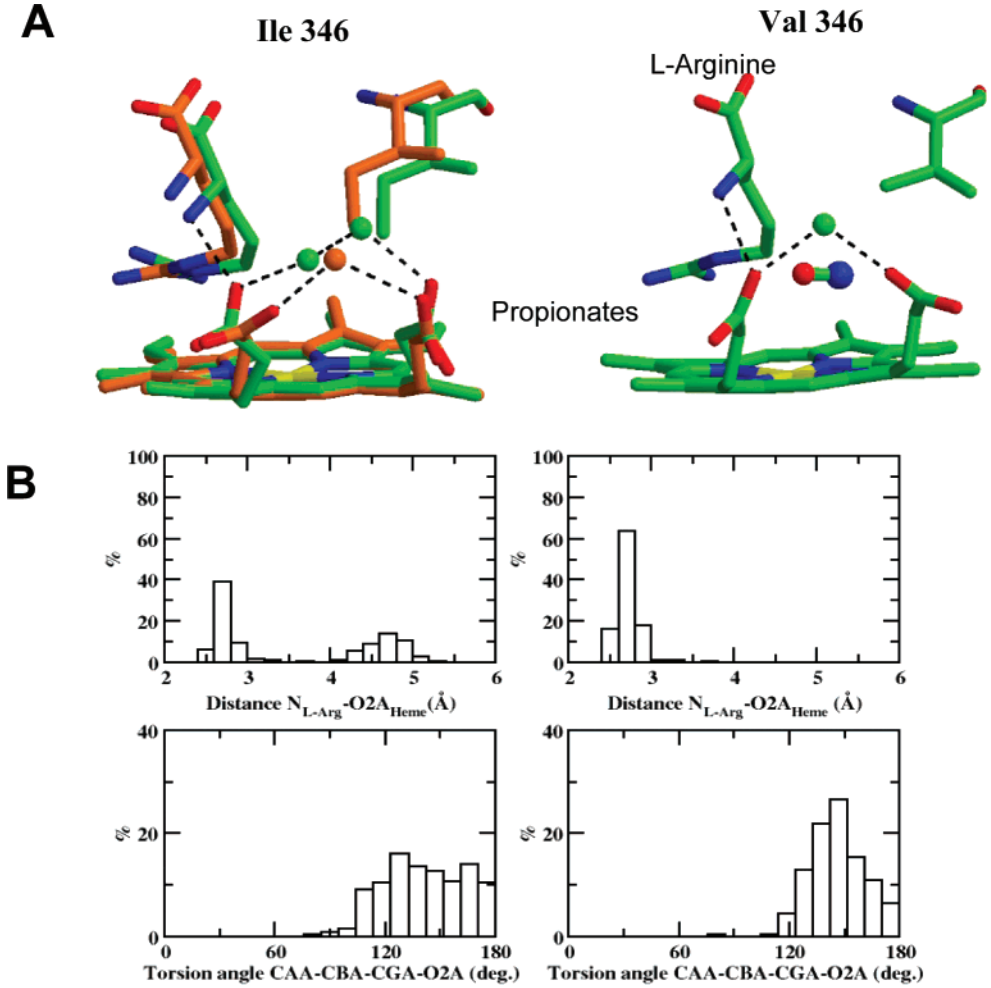

FIGURE 6: (A) Superposition of the two heme structures of V346I (left) with (green) and without (orange) a hydrogen bond between L-arginine and propionate after NO dissociation (not shown for clarity) obtained by molecular modeling. Comparison with the heme pocket of WT iNOS with the NO ligand after dissociation (right). The orange and green spheres represent the water molecule located in between the heme propionates. The BH_4 cofactor is not represented for clarity. (B) Fluctuations in the WT iNOS (right) and mutated V346I (left) structures shown by representative histograms: the upper graphs present the changes in the distance in Å between L-arginine and the heme propionate after NO dissociation. The abscissa is calculated as the percentage of the structures used; it represents an overall of 250 ps simulation with 1 ps steps. The bottom histograms show the variations of heme propionate A torsion angle.

propionates, and water molecule found in the simulations of V346I was consistent with a significant temperature effect in NO rebinding to V346I as compared to that in WT iNOS (Figure 5). The mutated protein was subject to larger thermal fluctuations than WT iNOS once the substrate site is filled. In particular, the larger temperature effect in the hundreds of picoseconds (reflected by changes in τ_2) on NO rebinding was consistent with enhanced change(s) in V346I as compared to WT iNOS (Table 2). These fluctuations only affected part of the heme pocket; WT iNOS and V346I had global structures with equivalent "mean disorder", as given by calculation of the rms: 1.7 and 1.5 Å, respectively. One ordered water molecule located in between the two propionate groups may mediate these interactions in V346I. Very similar H-bonding network to that found in this work linked the distal His-64, Arg-45 and the heme propionate through a water molecule in Mb, and Raman spectroscopy pointed out that NO binding affected this H-bonding via the propionate groups (*12*). These specific interactions afforded a pathway of information transmission from heme to protein induced by the dissociation of NO (or other diatomic ligands). Similar conformational changes in the distal site were found to be important for signal transduction to the kinase domain in sensory PAS proteins. These changes involved specific interactions between one propionate and a proximal histidine, disrupted upon binding of the (oxygen) ligand (*33*). Essential interactions between a heme propionate and a distal Arg220 locked the structure of the oxygen sensor FixLH and enhanced ligand discrimination (*34*). In cytochrome P450, Raman spectroscopy showed a strong coupling between the heme propionates, the substrate, and H-bonded amino acids, which was perturbed by mutation in the proximal heme side by steric effects. In the absence of the substrate, the propionate bending mode was insensitive to steric hindrance (*35*, *36*). Thus, the concerted effects of steric hindrance, substrate binding dynamics, and heme propionate rotation on the kinetics of ligand (re)binding was effective in V346I, with direct relation to function (*14*). Indeed, an observed rate of arginine binding of 80 s^{-1} (*37*) can be calculated on the basis of an estimate of 100 μM for the arginine concentration in human plasma (*38*); it should be faster than both the dissociation rate of citrulline (17 ± 2 s^{-1}) and the apparent rate of NO release from WT iNOS and V346I (2.3 ± 0.1 and 0.77 ± 0.03 s^{-1}, respectively) (*14*). This comparison suggested that the substrate binding site should not remain free of ligand (arginine or NOHA),

with high relevance to the control of NO release and iNOS function in vivo.

(b) Effect of the Presence of Filled/Empty Substrate Site on NO Rebinding; Comparison with Bacterial NOS. The present work emphasized a substrate-mediated steric effect. In constitutive NOS, the presence of a substrate affects NO binding to Fe(III) more than it does the binding to Fe(II). This is directly related to the linear binding mode in Fe(III)−NO, where a stronger spatial obstruction from the substrate would be experienced by a straight-up NO rather than a bent NO, as in Fe(II) (*39*). Thus, substrate binding was expected to influence the rate of NO geminate rebinding. In WT iNOS, Raman spectroscopy showed that the Fe−NO is distorted by BH_4 and arginine binding (*21*). Raman spectroscopy did not distinguish different Fe−NO bending modes in the ferric complexes of bsNOS with arginine and NOHA, despite the two structures of the ferric nitrosyl complex previously reported in the presence of NOHA (*17*, *35*). Figure 4 showed that, in the absence of substrate, almost identical kinetics was observed in WT iNOS and V346I. The abrogation of the effect of the mutation by an empty substrate site was consistent with our previous work on NO rebinding in the ferric complexes of the bacterial NOS-like proteins from *S. aureus* and *B. anthracis* (*20*). The very similar rebinding kinetics of NO in these proteins (*20*), especially in the first 500 ps in the absence of arginine, suggested a very similar heme conformation "sensed" by NO. In contrast, large differences between the bacterial and mammalian enzymes were revealed by binding of the substrate. The potential role of the heme propionates and their H-bonds was previously suggested. These hypotheses are now confirmed by this work with WT iNOS and V346I, which also allows characterizing rigorously the distal point mutation. Temperature effects and molecular dynamics supported the active role of the substrate and propionates in mediating the steric effect of the V346I mutation with large effects on function.

REFERENCES

1. Stuehr, D. J., Santolini, J., Wang, Z. Q., Wei, C. C., and Adak, S. (2004) Update on mechanism and catalytic regulation in the NO-synthases. *J. Biol. Chem. 279*, 36167−36170.
2. Alderton, W. K., Cooper, C. E., and Knowles, R. G. (2001) Nitric oxide synthases: Structure, function and inhibition. *Biochem. J. 357*, 593−615.
3. Martin, J. L., and Vos, M. H. (1992) Femtosecond biology. *Annu. Rev. Biophys. Biomol. Struct. 21*, 199−222.
4. Brunori, M., Vallone, B., Cutruzzola, F., Travaglini-Allocatelli, C., Berendzen, J., Chu, K., Sweet, R. M., and Schlichting, I. (2000) The role of cavities in protein dynamics: Crystal structure of a photolytic intermediate of a mutant myoglobin. *Proc. Natl. Acad. Sci. U.S.A. 97*, 2058−2063.
5. Wade, R. C., Winn, P. J., Schlichting, I., and Sudarko (2004) A survey of active site access channels in cytochromes P450. *J. Inorg. Biochem. 98*, 1175−1182.
6. Brunori, M., Bourgeois, D., and Vallone, B. (2004) The structural dynamics of myoglobin. *J. Struct. Biol. 147*, 223−234.
7. Ionascu, D., Gruia, F., Yu, X., Rosca, F., Beck, C., Demidov, A., Olson, J. S., and Champion, P. M. (2005) Temperature-dependent studies of NO recombination to the heme and heme proteins. *J. Am. Chem. Soc. 127*, 16921−16934.
8. Goldbeck, R. A., Bhaskaran, S., Ortega, C., Mendoza, J. L., Olson, J. S., Soman, J., Kliger, D. S., and Esquerra, R. M. (2006) Water and ligand entry in myoglobin: Assessing the speed and the extent of heme pocket hydration after CO photolysis. *Proc. Natl. Acad. Sci. U.S.A. 103*, 1254−1259.
9. Carlson, M. L., Regan, R. M., and Gibson, Q. H. (1996) Distal cavity fluctuations in myoglobin: Protein motion and ligand diffusion. *Biochemistry 35*, 1125−1136.
10. Nienhaus, K., Deng, P., Olson, J. S., Warren, J. J., and Nienhaus, G. U. (2003) Structural dynamics of myoglobin: Ligand migration and binding in valine 68 mutants. *J. Biol. Chem. 278*, 42532−42544.
11. Koyama, M., Neya, S., and Mizutani, Y. (2006) Role of heme propionates of myoglobin in vibrational energy relaxation. *Chem. Phys. Lett. 430*, 404−408.
12. Gao, Y., El-Mashtoly, S. F., Pal, B., Hayashi, T., Harada, K., and Kitagawa, T. (2006) Pathway of information from heme to protein upon ligand binding/dissociation in myoglobin revealed by UV resonance raman spectroscopy. *J. Biol. Chem. 281*, 24637−24646.
13. Zhang, Y., Fujisaki, H., and Straub, J. E. (2007) Molecular dynamics study on the solvent dependent heme cooling following ligand photolysis in carbonmoxy myoglobin. *J. Phys. Chem. B. 111*, 3243−3250.
14. Wang, Z. Q., Wei, C. C., Sharma, M., Pant, K., Crane, B. R., and Stuehr, D. J. (2004) A conserved Val to Ile switch near the heme pocket of animal and bacterial Nitric oxide synthase helps determine their distinct catalytic profiles. *J. Biol. Chem. 279*, 19018−19025.
15. Adak, S., Aulak, K. S., and Stuehr, D. J. (2002) Direct evidence for nitric oxide production by a nitric-oxide synthase-like protein from *Bacillus subtilis*. *J. Biol. Chem. 277*, 16167−16171.
16. Pant, K., Bilwes, A. M., Adak, S., Stuehr, D. J., and Crane, B. R. (2002) Structure of a nitric oxide synthase heme protein from *Bacillus subtilis*. *Biochemistry 41*, 11071−11079.
17. Pant, K., and Crane, B. R. (2006) Nitrosyl-heme structures of *Bacillus subtilis* nitric oxide synthase have implications for understanding substrate oxidation. *Biochemistry 45*, 2536−2544.
18. Adak, S., Bilwes, A. M., Panda, K., Hosfield, D., Aulak, K. S., McDonald, J. F., Tainer, J. A., Getzoff, E. D., Crane, B. R., and Stuehr, D. J. (2002) Cloning, expression, and characterization of a nitric oxide synthase protein from *Deinococcus radiodurans*. *Proc. Natl. Acad. Sci. U.S.A. 99*, 107−112.
19. Wang, Z. Q., Lawson, R. J., Buddha, M. R., Wei, C. C., Crane, B. R., Munro, A. W., and Stuehr, D. J. (2007) Bacterial flavodoxins support NO production by *Bacillus subtilis* nitric oxide synthase. *J. Biol. Chem. 282*, 2196−2202.
20. Gautier, C., Mikula, I., Nioche, P., Maratasek, P., Raman, C. S., and Slama-Schwok, A. (2006) Dynamics of NO rebinding to the heme domain of NO-synthase-like proteins from bacterial pathogens. *Nitric Oxide 15*, 312−327.
21. Li, D., Stuehr, D. J., Yeh, S. R., and Rousseau, D. L. (2004) Heme distortion by ligand−protein interactions in inducible nitric oxide synthase. *J. Biol. Chem. 279*, 26489−26499.
22. Gautier, C., Negrerie, M., Wang, Z. Q., Lambry, J. C., Stuehr, D. J., Collin, F., Martin, J. L., and Slama-Schwok, A. (2004) Dynamic regulation of the inducible nitric-oxide synthase by NO: Comparison with the endothelial isoform. *J. Biol. Chem. 279*, 4358−4365.
23. Petrich, J., Poyart, C., and Martin, J.-L. (1988) Photophysics and reactivity of heme proteins: A femtosecond absorption study of hemoglobin, myoglobin, and protoheme. *Biochemistry 27*, 4049−4060.
24. Press, W. H., Teukolsky, S. A., Vetterling, W. T., and Flannery, B. P. (1988) *Numerical Recipes*, Cambridge University Press, Cambridge, UK.
25. Li, H., Raman, C. S., Glaser, Blasko, E., Young, T. A., Parkinson, J. F., Whitlow, M., and Poulos, T. L. (1999) Crystal structures of zinc-free and -bound heme domain of human inducible nitric-oxide synthase. Implications for dimer stability and comparison with endothelial nitric-oxide synthase. *J. Biol. Chem. 274*, 21276−21284.
26. Lambry, J.-C., Vos, M. H., and Martin, J.-L. (1999) Molecular dynamics simulations of carbon monoxide dissociation from heme a_3 in cytochrome c oxydase from *Paracoccus denitrificans*. *J. Phys. Chem. A. 103*, 10132−10137.
27. Mewly, M., Becker, O. M., Stote, R., and Karplus, M. (2002) NO rebinding to myoglobin: A reactive molecular dynamics study. *Biophys. Chem. 98*, 1−2.
28. Salard, I., Mercey, E., Rekka, E., Boucher, J.-L., Nioche, P., Mikula, I., Martasek, P., Raman, C. S., and Mansuy, D. (2006) Analogies and surprising differences between recombinant nitric-oxide like proteins from *Staphylococcus aureus* and *Bacillus anthracis* in their interactions with L-arginine analogs and iron ligands. *J. Inorg. Chem. 100*, 2024−2033.
29. Abou-Soud, H., Wu, C., Ghosh, D. K., and Stuehr, D. J. (1998) Stopped-flow analysis of CO and NO binding to inducible nitric oxide synthase, *Biochemistry 37*, 3777−86.

30. Crane, B. R., Arvai, A. S., Ghosh, S., Getzoff, E. D., Stuehr, D. J., and Tainer, J. A. (2000) Structures of the *N*(omega)-hydroxy-L-arginine complex of inducible nitric oxide synthase oxygenase dimer with active and inactive pterins. *Biochemistry 39* (16), 4608−21.
31. Ghosh, D. K., and Salerno, J. C. (2003) NOS: Domain structure, alignment in enzyme function and control. *Frontiers Biosci. 8*, D193−209.
32. Peterson, E. S., Friedman, J. M., Chien, E. Y., and Sligar, S. G. (1998) Functionnal implications of the proximal hydrogen-bonding network in myoglobin; a resonance raman and kinetic study of Leu89, Ser92, His97, and F6helix swap mutants. *Biochemistry 37*, 12301−12319.
33. Uchida, T., Sato, E., Sato, A., Sagami, I., Shimizu, T., and Kitagawa, T. (2005) CO-dependent activity-controlling mechanism of heme-containing CO-sensor protein, neuronal PAS domain protein-2. *J. Biol. Chem. 280*, 21358−21368.
34. Balland, V., Bouzhir-Sima, L., Mallart, A. E., Boussac, A., Vos, M. H., Liebl, U., and Mattioli, T. A. (2006) Functional implications of the propionate 7−arginine 220 interactions in the FixLH oxygen sensor from *Bradyhizobium japonicum*. *Biochemistry 45*, 2072−2084.
35. Chartier, F. J., and Couture, M. (2007) Interactions between substrates and haem-bound NOS of ferric and ferrous bacterial nitric oxide synthases. *Biochem. J. 401*, 235−45.
36. Chen, Z., Ost, T. W. B., and Schelvis, J. P. M. (2004) Phe393 mutants of cytochrome P450 BM3 with modified heme redox potentials have altered heme vinyl and propionate conformations. *Biochemistry 43*, 1798−1808.
37. Santolini, J., Meade, A. L., and Stuehr, D. J. (2001) A kinetic simulation model that describes catalysis and regulation in nitric oxide synthase *J. Biol. Chem. 276*, 1233−43.
38. Boeger, R. H (2004) Asymetric dimethylarginine, an endogenous inhibitor of nitric oxide synthase, explains the "L-arginine paradox" and acts as a novel cardiovascular risk factor *J. Nutr. 134*, 2842S−47s.
39. Li, H., Igarashi, J., Jamal, J., Yang, W., and Poulos, T. L. (2006) Structural studies of constitutive nitric oxide synthases with diatomic ligands bound. *J. Inorg. Chem. 11*, 753−768.

BI701567H